Monthly Notices
of the
ROYAL ASTRONOMICAL SOCIETY

MNRAS **470,** 4163–4167 (2017)
Advance Access publication 2017 June 7

doi:10.1093/mnras/stx1397

Non-thermal photons and direct photodissociation of H_2, HD and HeH^+ in the chemistry of the primordial Universe

C. M. Coppola,[1,2★] M. V. Kazandjian,[3] D. Galli,[2★] A. N. Heays[3,4★] and E. F. van Dishoeck[3,5]

[1]*Dipartimento di Chimica, Università degli Studi di Bari, Via Orabona 4, I-70126 Bari, Italy*
[2]*INAF-Osservatorio Astrofisico di Arcetri, Largo E. Fermi 5, I-50125 Firenze, Italy*
[3]*Leiden Observatory, Leiden University, PO Box 9513, NL-2300 RA Leiden, the Netherlands*
[4]*LERMA, Observatoire de Paris, PSL Research University, CNRS, Sorbonne Universités, UPMC Univ. Paris 06, F-92190 Meudon, France*
[5]*Max-Planck-Institut fur extraterrestriche Physik, Postfach 1312, D-85741 Garching, Germany*

Accepted 2017 June 3. Received 2017 May 26; in original form 2017 May 22

ABSTRACT

Non-thermal photons deriving from radiative transitions among the internal ladder of atoms and molecules are an important source of photons in addition to thermal and stellar sources in many astrophysical environments. In the present work, the calculation of reaction rates for the direct photodissociation of some molecules relevant in early Universe chemistry is presented; in particular, the calculations include non-thermal photons deriving from the recombination of primordial hydrogen and helium atoms for the cases of H_2, HD and HeH^+. New effects on the fractional abundances of chemical species are investigated and the fits for the HeH^+ photodissociation rates by thermal photons are provided.

Key words: molecular processes – early Universe.

1 INTRODUCTION

Photodissociation processes represent important channels to destroy molecules in several astrophysical environments; the mechanisms through which they occur and the effects on the chemistry deeply depend on the chemical species involved and on the features of the radiation field these molecules are embedded in. For example, photodissociation due to UV photons produced by the interaction of cosmic rays with dense interstellar clouds has been reported in the literature (Prasad & Tarafdar 1983; Sternberg, Dalgarno & Lepp 1987; Heays, Bosman & van Dishoeck 2017) and the effects of such UV flux on the chemistry have been described for several chemical species (Gredel, Lepp & Dalgarno 1987; Gredel et al. 1989; Heays et al. 2014). Another example is represented by the X-ray spectra emitted by high-mass young stellar objects (YSOs) that are usually fitted with the emission spectrum of an optically thin thermal plasma (Hofner & Churchwell 1997) and that has been used to describe the chemistry in the envelopes around YSOs (Stäuber et al. 2006). On the other hand, photodissociation can occur following specific dynamical pathways according to the features of the potential energy surfaces describing the possible electronic states of the molecules themselves. In particular, direct photodissociation, predissociation and spontaneous radiative photodissociation are described as the main ways to photodestroy small molecules [e.g. contribution by van Dishoeck in Millar & Williams (1988) and van Dishoeck & Visser (2014)]; according to the dynamics, different features in the photodissociation cross-sections can be observed. Eventually, considering both the radiation field and the dynamics of the photodissociation processes, additional terms can be calculated other than the thermal emission contribution to the reaction rate of photoprocesses.

When moving to the early Universe case, non-thermal radiation fields can arise as a result of different mechanisms such as matter/antimatter annihilation, decaying relic/dark matter particles, dissipation of acoustic waves (see e.g. Chluba & Sunyaev 2012), radiative cascade of H_2 (Coppola et al. 2012) among others. They are also called 'distortion photons' because of their departure from the Planckian shape of the cosmic microwave background spectrum. Among these additional radiation fields, the most relevant for its effect on the chemistry of the primordial Universe and for the level of accuracy with which it has been modelled is represented by the spectrum deriving from the recombination processes of H and He in the so-called epoch of recombination (Chluba & Sunyaev 2006; Chluba, Vasil & Dursi 2010; Chluba & Thomas 2011). In fact, because of the adiabatic expansion of the Universe and the effective Compton scattering, the temperature of the matter dropped, allowing for the first bound atomic states to form. The effect of non-thermal photons on the early Universe chemistry has been studied in several papers, both in terms of changes in the fractional abundances of species (e.g. Hirata & Padmanabhan 2006) or in their optical depths (e.g. Switzer & Hirata 2005). In particular, Coppola et al. (2013) presented a modified version of the chemistry in the primordial Universe, where the effect of non-thermal photons was investigated on two photodestruction processes that are relevant for the chemistry of

★ E-mail: carla.coppola@uniba.it (CMC); galli@arcetri.astro.it (DG); heays@strw.leidenuniv.nl (ANH)

H_2, namely the photodissociation of H_2^+ and the photodetachment of H^-.

In the present work, we focus on the effect of non-thermal photons on the photodissociation of the molecular species that are of interest for the primordial Universe. The calculations presented by Coppola et al. (2013) will be here extended to the direct photodissociation of H_2, HD and HeH^+. Although quite simple systems, they represent the key molecular species present in the early Universe chemistry; indeed, while H_2 and HD are connected to the cooling of the gas down to few tens of kelvins in the low-metallicity environment present at high redshifts (e.g. Galli & Palla 1998; Lepp, Stancil & Dalgarno 2002; Dalgarno 2005), HeH^+ contributes to the opacity and optical properties of the primordial gas itself (e.g. Schleicher et al. 2008).

This paper is organized as follows: in Section 2, the formalism used for the description and implementation of non-thermal photons in the chemical kinetics is introduced, and the processes investigated are listed. The quantum dynamical features of each channel are described, and references for the used cross-sections are provided. In Section 3, the resulting non-thermal rate coefficients are shown and the effects on the chemical kinetics are discussed and reported.

2 FORMULATION OF THE PROBLEM

2.1 Distortion photons and non-thermal rate coefficient

Radiative transitions in any quantum system between higher, i, and lower, j, internal energy levels (or a lower energy continuum) are associated with the emission of a photon, causing a spectral distortion of specific intensity $\Delta I_{ij}(\nu)$. The observed frequency, ν, of a photon emitted at redshift $z_{\rm em}$ and observed at redshift z is related to its rest-frame frequency, ν_{ij}, according to $\nu = \nu_{ij}(1+z)/(1+z_{\rm em})$, assuming a narrow line profile. The spectral distortion produced by the emission process at $z_{\rm em}$ and observed at redshift $z < z_{\rm em}$ can be written as (e.g. Rubiño-Martín, Chluba & Sunyaev 2008)

$$\Delta I_{ij}^{z}(\nu) = \left(\frac{hc}{4\pi}\right) \frac{\Delta R_{ij}(z_{\rm em})(1+z)^3}{H(z_{\rm em})(1+z_{\rm em})^3}, \quad (1)$$

where $H(z) = H_0[\Omega_{\rm r}(1+z)^4 + \Omega_{\rm m}(1+z)^3 + \Omega_{\rm k}(1+z)^2 + \Omega_\Lambda]^{1/2}$ is the Hubble function and ΔR_{ij} is related to the population of the ith and jth levels by

$$\Delta R_{ij} = p_{ij} A_{ij} N_i \frac{e^{h\nu_{ij}/k_{\rm B}T_{\rm r}}}{e^{h\nu_{ij}/k_{\rm B}T_{\rm r}} - 1} \left[1 - \frac{g_i N_j}{g_j N_i} e^{-h\nu_{ij}/k_{\rm B}T_{\rm r}}\right], \quad (2)$$

where p_{ij} is the Sobolev escape probability, g_i and g_j are the degeneracy of upper and lower levels, respectively (both factors are equal to one in the case of pure vibration transitions), A_{ij} is the Einstein coefficient of the transition and $T_{\rm r} = 2.726(1+z_{\rm em})$ K (Fixsen 2009).

Eventually, the total contribution of spectral distortions to the rate of a reaction with photons at a given redshift, z, can be evaluated by integration over the photon distribution:

$$k_{\rm ph}(z) = 4\pi \int_0^\infty \frac{\sigma(\nu)}{h\nu} \left[B_z(\nu) + \sum_{i\to j} \Delta I_{ij}^{z}(\nu)\right] {\rm d}\nu. \quad (3)$$

In this equation, $\sigma(\nu)$ represents the cross-section of the process as a function of frequency and $B_z(\nu)$ is the Planck distribution at $T_{\rm r}$ corresponding to the redshift z at which the reaction rate is calculated. In Fig. 1, the spectra for the non-thermal and thermal photons

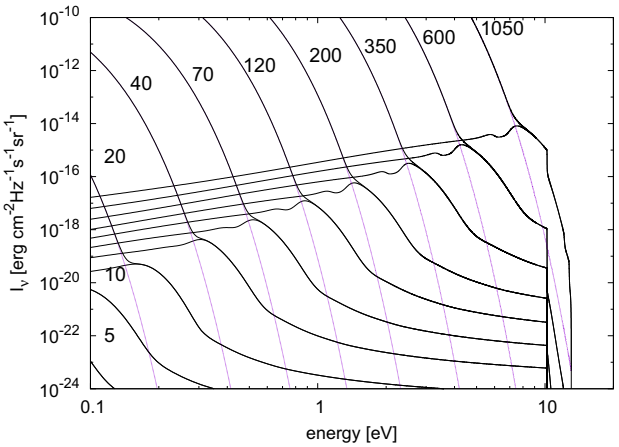

Figure 1. Thermal and non-thermal spectra at different redshift z. Together with the Planck distribution at different radiation temperatures (purple dotted curves, corresponding to the redshift values reported in the figure), the non-thermal contributions are reported. The latter derive both from primordial atomic recombination of H and He and H_2 radiative cascade.

are reported for different values of the redshift; the calculations performed in this paper have been based on these spectra. Additional details on non-thermal photons distribution can be found in Coppola et al. (2013).

2.2 Molecular species

In the following, a description of the photodissociation processes and molecular species modelled in the present work is given.

2.2.1 H_2

The photodissociation of H_2 proceeds by two dynamical mechanisms; first, the Solomon process consists of a two-step pathway with bound–bound resonant absorption through the Lyman and Werner bands followed by fluorescent decay into the continuum of the ground electronic state:

$$H_2^{(X;v,j)} + h\nu \rightarrow H_2^{(B/C;v',j')} \rightarrow H(1s) + H(1s) + h\nu. \quad (4)$$

The cross-sections show a peculiar peaked behaviour at the energy corresponding to the energies of the emitted photons (e.g. Mentall & Guyon 1977). The Solomon process has been always treated as the main photodestruction channel of H_2 in studies of several environments (Stecher & Williams 1967; Abgrall et al. 1992; Abgrall, Roueff & Drira 2000), including the early Universe case (Galli & Palla 1998; Lepp et al. 2002; Dalgarno 2005). Although reaction (4) represents the main channel though which photodissociation occurs, it has been shown that the direct continuum photodissociation process

$$H_2^{(X;v,j)} + h\nu \rightarrow H(1s) + H(2p) \quad (5)$$

can affect the total rate coefficients, for example, in the case of interstellar clouds (Shull 1978) and in the early Universe chemistry (Coppola et al. 2011a). Several authors have calculated the cross-sections for process (5) (Allison & Dalgarno 1969; Glass-Maujean 1986; Zucker & Eyler 1986); more recently, Gay et al. (2012) provided rovibrationally resolved cross-sections. They are available at the website http://www.physast.uga.edu/ugamop/, together with the energy levels. The overall H_2 photoexcitation-emission cross-section is highly structured, being a mixture of Doppler-limited line

emission and an underlying continuum due to processes (4) and (5), respectively.

2.2.2 *HD*

HD photodissociation is homologous to the H_2 case. A cross-section is calculated by Allison & Dalgarno (1969), though only vibrationally resolved. In the present work, the rotational quantum number of the available cross-sections is assumed to be equal to zero.

2.2.3 *HeH$^+$*

The photodissociation of HeH^+ has been extensively studied both from a theoretical and experimentalist point of view (Loreau et al. 2011; Gay et al. 2012; Urbain et al. 2012), also in the case of excited electronic states (Miyake, Gay & Stancil 2011; Loreau et al. 2013). In this case, the photodissociation is dominated by two processes:

$$HeH^+(X^1\Sigma^+, v, J) + h\nu \rightarrow He^+(1s) + H(1s)(A^1\Sigma^+) \quad (6)$$

$$HeH^+(X^1\Sigma+, v, J) + h\nu \rightarrow He(1s^2) + H^+(X^1\Sigma^+). \quad (7)$$

In the following, these are referred to as $A \leftarrow X$ and $X \leftarrow X$ photodissociation, respectively. As in the case of direct photodissociation of H_2, rovibrationally resolved cross-sections and energy levels are available at the website http://www.physast.uga.edu/ugamop/; the details on the calculations can be found in the work by Miyake et al. (2011). These two channels have been previously inserted in chemical networks describing the formation and destruction of primordial molecules (e.g. Galli & Palla 1998; Lepp et al. 2002; Schleicher et al. 2008).

3 RESULTS

The main results concern both photodissociation rates and fractional abundances in the context of early Universe chemistry. In the following, the results are described according to the chemical species.

3.1 Reaction rates

3.1.1 *H_2 and HD*

In Fig. 2, thermal and non-thermal reaction rates for the process of direct photodissociation calculated according to equation (3) are shown, for H_2 and HD (top and bottom panels, respectively) as a function of redshift. The presence of extra photons produced by the primordial recombination of H and He results in the formation of a non-thermal tail in the reaction rate. The value of the redshift at which the crossing-over between non-thermal and the thermal reaction rate appears is $z \sim 1300$; at this z, the radiation temperature is $T_r \sim 3545$ K. The curves referred to as C11 correspond to the fits provided by Coppola et al. (2011a).

3.1.2 *HeH$^+$*

In Fig. 3, the reaction rates for direct photodissociation of HeH^+ are shown, separately for the cases of $A \leftarrow X$ and $X \leftarrow X$. It is possible to see two important features: first, photodissociation rates from thermal photons are quite different from the usually adopted fits (e.g. Schleicher et al. 2008, referred to as S08 in the figure, and Galli & Palla 1998), which were derived by detailed balance on the data for radiative association of He and H^+ and H and He^+.

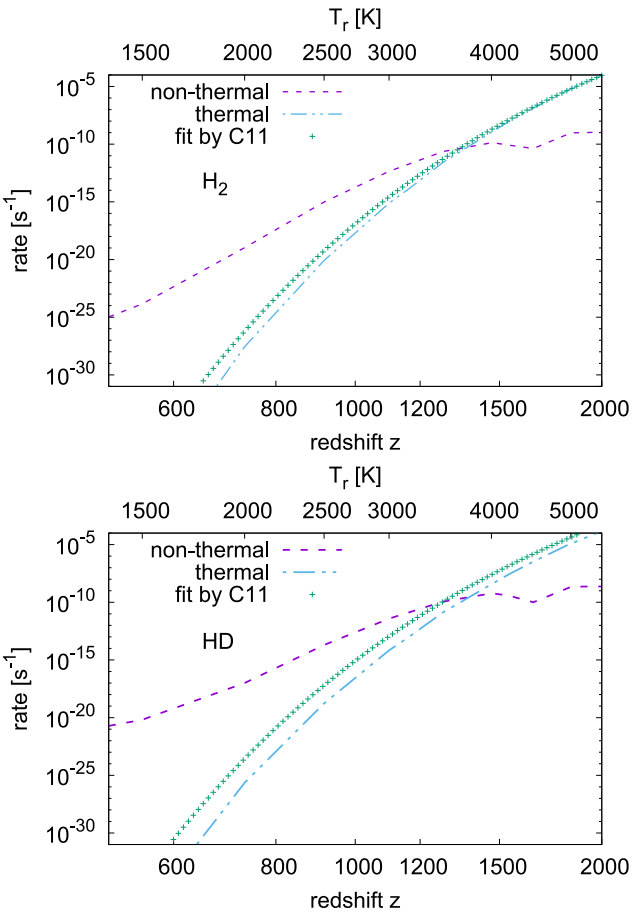

Figure 2. Photodissociation rates as a function of redshift for direct photodissociation of H_2 (top panel) and HD (bottom panel). Both rates calculated adopting a thermal radiation spectrum and non-thermal photons are shown. Comparison with data calculated by Coppola et al. (2011a, reported as C11 in the key) is provided.

Secondly, redshift values at which photodissociation rates from non-thermal photons become greater than the thermal contribution are significantly different in the two cases; in the case of the process $A \leftarrow X$, this departure happens at $z \sim 1100$ and at $z \sim 200$ for the process $X \leftarrow X$. Then, the radiation temperatures are quite different, respectively $T_r \sim 3000$ K and $T_r \sim 550$ K.

3.2 Fractional abundances

The calculated direct photodissociation rates calculated by considering both thermal and non-thermal emission with the available cross-sections have been implemented in a time-dependent chemical network (e.g. Galli & Palla 1998, 2013; Coppola et al. 2011b; Longo et al. 2011). The presence of non-thermal photons does not significantly affect the fractional abundances of the chemical species of interest; this result is qualitatively expected from comparing the values at which the departure from thermal to non-thermal features occurs and the maxima in the cross-sections.

A significant deviation follows from the introduction of the direct process of photodissociation for H_2 and HD (in addition to the Solomon processes) at high values of redshift, where differences up to four orders of magnitude can be appreciated (see Fig. 4). Although significant, this result does not affect the successive phases of chemical evolution, which are mainly controlled by formation

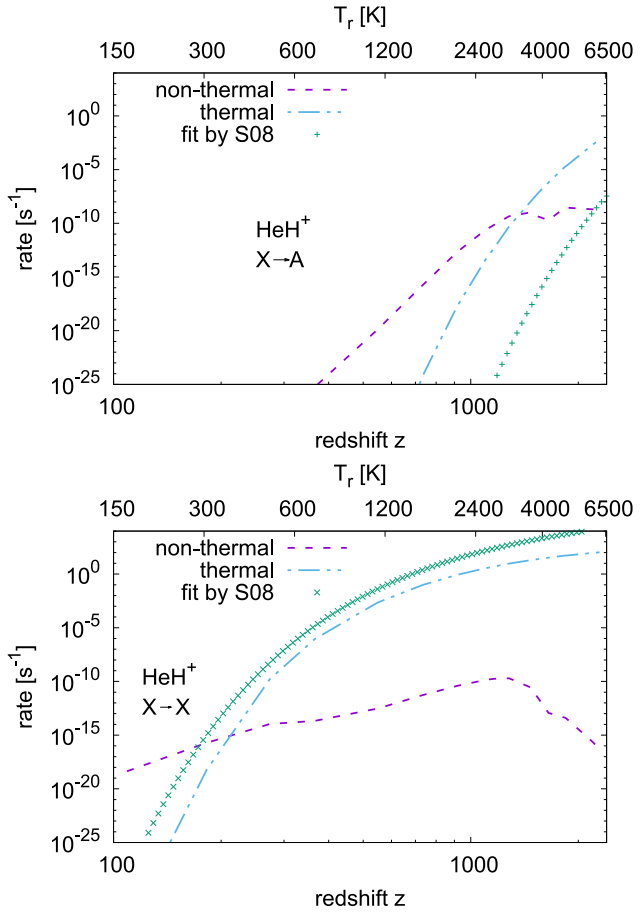

Figure 3. Photodissociation rates for HeH^+: thermal and non-thermal contribution. Top panel: transition $A \leftarrow X$; bottom panel: transition $X \leftarrow X$. The blue curve is the thermal contribution calculated in the present work adopting the cross-sections by Gay et al. (2012) while the green curve represents the contribution of non-thermal photons to the reaction rate. The crosses represent fits implemented by Schleicher et al. (2008).

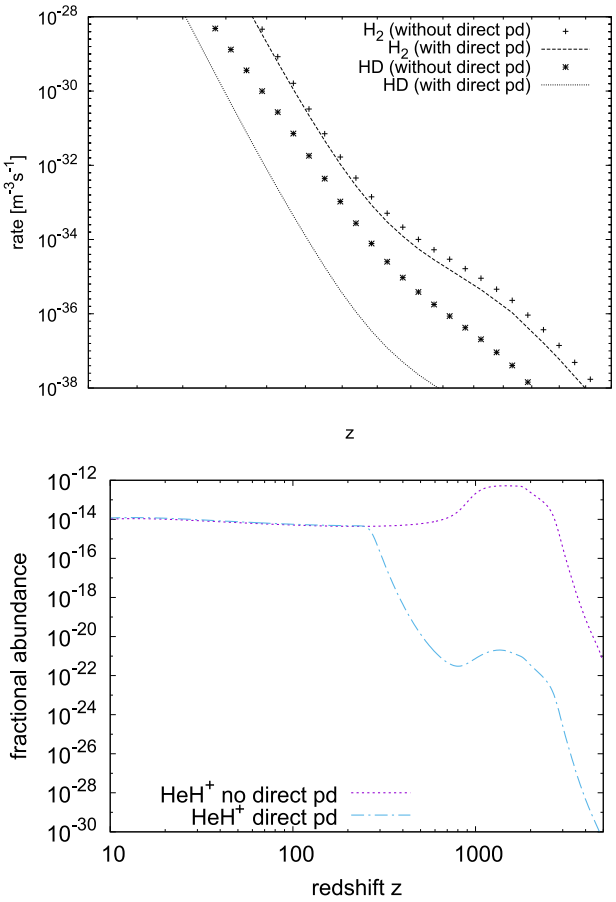

Figure 4. HeH^+ fractional abundances: with and without the contribution of direct photodissociation; top panel: H_2 and HD, bottom panel: HeH^+.

processes occurring at lower redshifts (H_2^+ channel followed by the H^- one).

4 CONCLUSIONS

In the present work, the effect of non-thermal photons on the direct photodissociation of three molecules in the context of early Universe chemistry has been investigated. There is no effect on molecular abundances at low redshifts, but some large changes occur at higher z. Such effects agree with estimates performed by taking into account on one hand the thresholds for these chemical processes and, on the other hand, the radiation temperature at which they are expected to become significant. In the case of H_2 and HD, for example, the energy threshold is quite high; consequently, the direct photodissociation is expected to play a role at high values of z, as confirmed by the present simulations. Moreover, the contribution to the photodissociation rates from thermal and non-thermal photons has been provided, showing the ranges at which each term dominates. Updated fits for the direct photodissociation rates of HeH^+ as a function of radiation temperature are provided in Appendix A; moreover, a human readable (ASCII) file containing the rates due to non-thermal photons is available as supplementary online material.

ACKNOWLEDGEMENTS

CMC and DG acknowledge the discussions within the international team #272 lead by CMC 'EUROPA – Early Universe: Research on Plasma Astrochemistry' at ISSI (International Space Science Institute) in Bern. CMC also greatly acknowledges Regione Puglia for the project 'Intervento cofinanziato dal Fondo di Sviluppo e Coesione 2007-2013 – APQ Ricerca Regione Puglia – Programma regionale a sostegno della specializzazione intelligente e della sostenibilità sociale ed ambientale – FutureInResearch'.

REFERENCES

Abgrall H., Le Bourlot J., Pineau des Forêts G., Roueff E., Flower D. R., Heck L., 1992, A&A, 253, 525
Abgrall H., Roueff E., Drira I., 2000, A&AS, 141, 297
Allison A. C., Dalgarno A., 1969, At. Data, 1, 91
Chluba J., Sunyaev R. A., 2006, A&A, 458, 29
Chluba J., Sunyaev R. A., 2012, MNRAS, 419, 1294
Chluba J., Thomas R. M., 2011, MNRAS, 412, 748
Chluba J., Vasil G. M., Dursi L. J., 2010, MNRAS, 407, 599
Coppola C. M., Diomede P., Longo S., Capitelli M., 2011a, ApJ, 727, 37
Coppola C. M., Longo S., Capitelli M., Palla F., Galli D., 2011b, ApJS, 193, 7
Coppola C. M., D'Introno R., Galli D., Tennyson J., Longo S., 2012, ApJS, 199, 16
Coppola C. M., Galli D., Palla F., Longo S., Chluba J., 2013, MNRAS, 434, 114
Dalgarno A., 2005, J. Phys.: Conf. Ser., 4, 10
Fixsen D. J., 2009, ApJ, 707, 916

Galli D., Palla F., 1998, A&A, 335, 403
Galli D., Palla F., 2013, ARA&A, 51, 163
Gay C. D., Abel N. P., Porter R. L., Stancil P. C., Ferland G. J., Shaw G., van Hoof P. A. M., Williams R. J. R., 2012, ApJ, 746, 78
Glass-Maujean M., 1986, Phys. Rev. A, 33, 342
Gredel R., Lepp S., Dalgarno A., 1987, ApJ, 323, L137
Gredel R., Lepp S., Dalgarno A., Herbst E., 1989, ApJ, 347, 289
Heays A. N., Visser R., Gredel R., Ubachs W., Lewis B. R., Gibson S. T., van Dishoeck E. F., 2014, A&A, 562, A61
Heays A. N., Bosman A. D., van Dishoeck E. F., 2017, A&A
Hirata C. M., Padmanabhan N., 2006, MNRAS, 372, 1175
Hofner P., Churchwell E., 1997, ApJ, 486, L39
Lepp S., Stancil P. C., Dalgarno A., 2002, J. Phys. B: At. Mol. Opt. Phys., 35, R57
Longo S., Coppola C. M., Galli D., Palla F., Capitelli M., 2011, Rend. Lincei, 22, 119
Loreau J., Lecointre J., Urbain X., Vaeck N., 2011, Phys. Rev. A, 84, 053412
Loreau J., Vranckx S., Desouter-Lecomte M., Vaeck N., Dalgarno A., 2013, J. Phys. Chem. A, 117, 9486
Mentall J. E., Guyon P. M., 1977, J. Chem. Phys., 67, 3845
Millar T. J., Williams D. A. eds, 1988, Astrophysics and Space Science Library, Vol. 146, Rate Coefficients in Astrochemistry. Kluwer, Dordrecht, p. 49
Miyake S., Gay C. D., Stancil P. C., 2011, ApJ, 735, 21
Prasad S. S., Tarafdar S. P., 1983, ApJ, 267, 603
Rubiño-Martín J. A., Chluba J., Sunyaev R. A., 2008, A&A, 485, 377
Schleicher D. R. G., Galli D., Palla F., Camenzind M., Klessen R. S., Bartelmann M., Glover S. C. O., 2008, A&A, 490, 521
Shull J. M., 1978, ApJ, 219, 877
Stäuber P., Jørgensen J. K., van Dishoeck E. F., Doty S. D., Benz A. O., 2006, A&A, 453, 555
Stecher T. P., Williams D. A., 1967, ApJ, 149, L29
Sternberg A., Dalgarno A., Lepp S., 1987, ApJ, 320, 676
Switzer E. R., Hirata C. M., 2005, Phys. Rev. D, 72, 083002
Urbain X., Lecointre J., Loreau J., Vaeck N., 2012, J. Phys.: Conf. Ser., 388, 022107
van Dishoeck E. F., Visser R., 2014, Laboratory Astrochemistry: From Molecules through Nanoparticles to Grains. Wiley-VCH, Weinheim, p. 229
Zucker C. W., Eyler E. E., 1986, J. Chem. Phys., 85, 7180

SUPPORTING INFORMATION

Supplementary data are available at *MNRAS* online.

Please note: Oxford University Press is not responsible for the content or functionality of any supporting materials supplied by the authors. Any queries (other than missing material) should be directed to the corresponding author for the article.

APPENDIX A: FITS

The calculations reported in this paper concerning HeH^+ have been performed using the cross-sections of Miyake et al. (2011). For convenience, we provide an empirical form of the thermal rates, both for the transition $A \leftarrow X$ and $X \leftarrow X$ to the analytical expression:

$$k(T_r) = aT_r^b \exp(-c/T_r). \quad \text{(A1)}$$

The values of the parameters in both cases are reported in Table A1, together with the ranges of radiation temperature for which the fits are valid.

Table A1. HeH^+ direct photodissociation reaction rates: updated fits for the thermal contribution as a function of T_r. The ranges for which the fits are accurate are reported in the last column.

	Thermal (s^{-1})	Range (K)
$HeH^+(X^1\Sigma^+, v, J) + h\nu \rightarrow He^+(1s) + H(1s)(A^1\Sigma^+)$		[200–6000]
	$a = 273\,518$	
	$b = 0.623\,525$	
	$c = 144\,044$ [K]	
$HeH^+(X^1\Sigma +, v, J) + h\nu \rightarrow He(1s^2) + H^+(X^1\Sigma^+)$		
	$a = 2.030\,97 \times 10^8$	[200–7000]
	$b = -1.202\,81$	
	$c = 24\,735$ [K]	

This paper has been typeset from a TEX/LATEX file prepared by the author.